Pediatr Surg Int (2014) 30:223–231
DOI 10.1007/s00383-013-3451-0

ORIGINAL ARTICLE

Analysis of blood and lymph vascularization patterns in tissue-engineered human dermo-epidermal skin analogs of different pigmentation

Agnieszka S. Klar · Sophie Böttcher-Haberzeth · Thomas Biedermann · Clemens Schiestl · Ernst Reichmann · Martin Meuli

Published online: 22 December 2013

Abstract
Purpose Bioengineered dermo-epidermal skin analogs containing melanocytes represent a promising approach to cover large skin defects including restoration of the patient's own skin color. So far, little is known about the development of blood and lymphatic vessels in pigmented skin analogs after transplantation. In this experimental study, we analyzed the advancement and differences of host blood and lymphatic vessel ingrowth into light- and dark-pigmented human tissue-engineered skin analogs in a rat model.
Methods Keratinocytes, melanocytes, and fibroblasts from light- and dark-pigmented skin biopsies were isolated, cultured, and expanded. For each donor, melanocytes and keratinocytes were seeded in ratios of 1:1, 1:5, and 1:10 onto fibroblast-containing collagen gels. The skin analogs were subsequently transplanted onto full-thickness wounds of immuno-incompetent rats and quantitatively analyzed for vascular and lymphatic vessel density after 8 and 15 weeks.
Results The skin analogs revealed a significant difference in vascularization patterns between light- and dark-pigmented constructs after 8 weeks, with a higher amount of blood vessels in light compared to dark skin. In contrast, no obvious difference could be detected within the light- and dark-pigmented group when varying melanocyte/keratinocyte ratios were used. However, after 15 weeks, the aforementioned difference in blood vessel density between light and dark constructs could no longer be detected. Regarding lymphatic vessels, light and dark analogs showed similar vessel density after 8 and 15 weeks, while there were generally less lymphatic than blood vessels.
Conclusion These data suggest that, at least during early skin maturation, keratinocytes, melanocytes, and fibroblasts from different skin color types used to construct pigmented dermo-epidermal skin analogs have distinct influences on the host tissue after transplantation. We speculate that different VEGF expression patterns might be involved in this disparate revascularization pattern observed.

Keywords Melanocytes · Melanocyte/keratinocyte ratio · Tissue-engineering · Light-/dark-pigmented skin analog · Skin vascularization · Blood vessels · Lymphatic vessels · Rat model

Introduction

The therapy of large full-thickness skin wounds, as e.g., in massive burns, is often difficult due to their complex systemic impact and also lack of sufficient autologous donor skin. Theoretically, tissue-engineered full-thickness skin analogs offer an important alternative to conventional autologous skin grafts. For several years, our laboratory has made substantial efforts to develop and characterize a tissue-engineered dermo-epidermal skin equivalent [1–5]. Most recently, we reconstituted pigmented dermo-

A. S. Klar and S. Böttcher-Haberzeth contributed equally to this paper.

A. S. Klar · S. Böttcher-Haberzeth · T. Biedermann · E. Reichmann
University Children's Hospital Zurich, Tissue Biology Research Unit, Zurich, Switzerland

S. Böttcher-Haberzeth · C. Schiestl · M. Meuli (✉)
University Children's Hospital Zurich, Department of Surgery, Steinwiesstrasse 75, 8032 Zurich, Switzerland
e-mail: martin.meuli@kispi.uzh.ch

epidermal skin analogs from different pigmentation types and achieved very satisfactory in vivo results restoring the patients' native skin color [5]. This strategy holds promise for treatment of full-thickness skin defects as well as skin pigmentation disorders [6] in that the transplanted skin not only covers the defect, but also protects against ultraviolet radiation and provides the original skin color.

It has been shown, that the skin of light- and dark-pigmented individuals exhibits numerous intrinsic physiological differences. Montagna et al. reported that the epidermis of black skin has more and larger singly distributed melanosomes in keratinocytes, and contains more cell layers in the stratum corneum than that of white skin [7]. The dermis of black skin demonstrates more collagen fibrils, glycoproteins, and larger, more numerous fibroblasts, as well as more apocrine and eccrine sweat glands than that of white skin [8]. Moreover, black skin shows a higher density of superficial (subepidermal) blood vessels as well as more numerous, larger lymphatic vessels and more nerve fibers than white skin [8]. Black subjects' skin is also less susceptible to cutaneous irritation induced by either chemicals or UV light and displays less erythema, less blood vessel reactivity, and cutaneous blood flow than white skin [9–12].

However, little is known about the development of blood and lymphatic vessels in tissue-engineered pigmented skin analogs of different pigmentation types after transplantation and, in particular, there is no data regarding the aforementioned physiologic differences between black and white skin.

In this experimental study, we investigated the differences of host blood and lymphatic vessel ingrowth into human tissue-engineered skin analogs derived from light- and dark-pigmented donor skin at 8 and 15 weeks after transplantation in a rat model.

Materials and methods

Human skin samples

The investigation was conducted according to Declaration of Helsinki principles and after acceptance of the ethic commission of the Canton Zurich. Children's parents gave informed consent to use skin samples. The human foreskin samples were obtained from light and dark skin pigmentation types from patients 1 to 16 years of age. Human epidermal keratinocytes, melanocytes, and dermal fibroblasts were isolated from the skin samples. Tissue samples for histological examinations were embedded in paraffin or in OCT compound (Sakura Finetek, Switzerland) and kept at −20 °C.

Isolation and culturing of primary cells

Keratinocytes and fibroblasts were isolated and cultured as described by Pontiggia et al. [4] and Biedermann et al. [13] and melanocytes as specified in Bottcher-Haberzeth et al. [5].

Preparation of tissue-engineered skin analogs

Transwell cell culture plates in six-well format containing inserts with 3.0 μm pore-size membranes (BD Falcon, Switzerland) were used to prepare skin analogs [3]. To reconstruct the dermal compartment, rat collagen type I was mixed with 0.2 ml neutralization buffer containing 0.15 M NaOH and with 1×10^5 human dermal fibroblasts (passage 1–3). After 10 min polymerization at room temperature and 45 min in an incubator at 37 °C, the dermal equivalents were grown for 7 days in Dulbecco's modified Eagle's (DMEM) medium enriched with 10 % FCS and Hepes (DMEM, Invitrogen, Switzerland). Subsequently, 5×10^5 keratinocytes and melanocytes (passage 1–3) of the corresponding donor skin were seeded in different ratios (melanocyte/keratinocytes 1:1, 1:5, or 1:10) onto dermal equivalents. The skin analogs were cultured for 1 week in a 1:5 mix of melanocyte growth medium (Promocell, Germany) and keratinocyte medium (SFM, Invitrogen, Switzerland) and subsequently transplanted.

Transplantation of cultured dermo-epidermal skin analogs

All animal studies have been approved by the local committee for experimental animal research (permission number: 76/2011). Immuno-deficient female nu/nu rats, 8–10 weeks old (Harlan Laboratories, Netherlands), were anesthetized as previously described [14, 15]. Full-thickness skin wounds were created on the backs of the rats. Subsequently, custom-made steel rings (diameter 2.6 cm) were sutured into the skin wounds using non-absorbable polyester sutures (Ethibond®, Ethicon, USA) and the skin analogs were sutured into those rings. Steel rings protected the skin analogs and prevented the closure of the wound by the surrounding rat skin. The transplants were then covered with a silicone foil (Silon-SES, BMS, USA), a polyurethane sponge (Ligasano, Ligamed, Austria), a cohesive conforming bandage (Sincohaft, Theo Frey AG, Switzerland), and tape as wound dressing. Dressing changes and photographic documentations were performed once per week. After 8 ($N = 20$) or 15 ($N = 9$) weeks the transplanted skin analogs were excised in toto and processed for paraffin- and cryosections.

Histological analysis

Paraffin sections (5 μm) were stained with hematoxylin and eosin (Sigma, Switzerland) to assess the histological morphology.

Immunohistochemical staining

Immunofluorescence staining was performed as described in Bottcher-Haberzeth et al. [15, 16]. Double immunofluorescence stainings were performed to visualize rat blood and/or lymphatic vessels (CD31 [clone TDL-3A12, 1:50, BD Pharmingen, Switzerland], LYVE1 [polyclonal, 1:200, Novus Biologicals, UK]), and human fibroblasts (CD90 [clone 5E10, 1:50, Dianova, Germany]). The human control skin samples were double stained for human CD31 [clone JC70A, 1:50, Dako, Switzerland], LYVE1 [clone ab10278, 1:200, Abcam, UK]), and human fibroblasts (CD90 [clone AS02, 1:50, Dianova, Germany]).

Pictures of immunofluorescence stainings were taken with a DXM1200F digital camera connected to a Nikon Eclipse TE2000-U inverted microscope. The device is equipped with Hoechst 33342-, FITC-, and TRITC-filter sets (Nikon AG, Switzerland; Software: Nikon ACT-1 vers. 2.70). Images were processed with Photoshop 7.0 (Adobe Systems Inc, Germany).

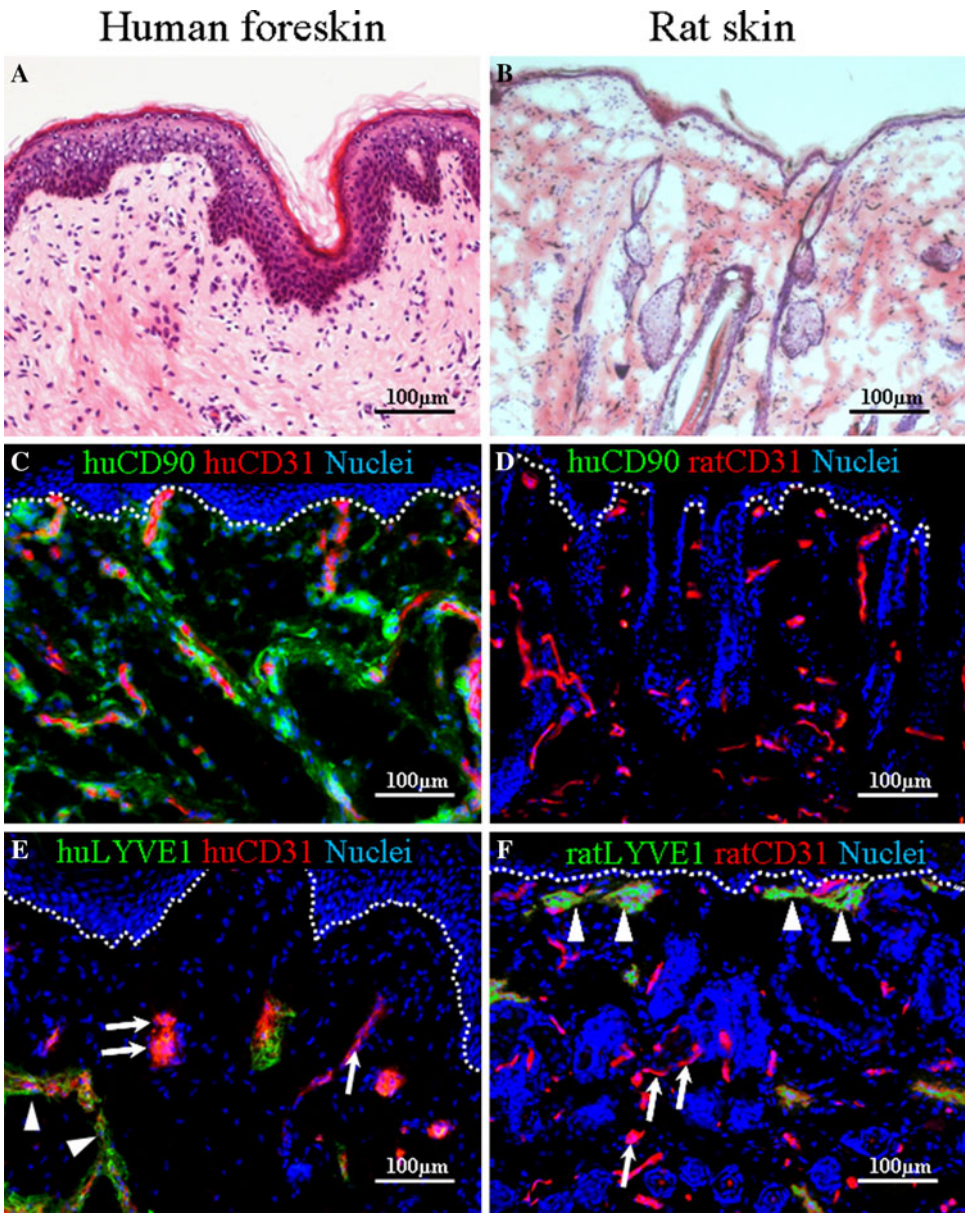

Fig. 1 Evaluation of normal human foreskin and rat back skin and the expression of blood- and lymphatic-specific markers. **a, b** Hematoxylin and eosin staining showing a comparison of normal human versus rat skin; rat skin reveals less layers in the epidermis and abundant hair follicles in the dermis. **c, d** Immunofluorescence double staining of human and rat skin with antibodies against human CD90 (staining of human dermal compartment, *green*) and against human and rat CD31 (staining of blood vessels, *red*). **e, f** Immunofluorescence double staining of human and rat skin with antibodies against human and rat LYVE1 (lymphatic vessels, *green*) and against human and rat CD31 (blood vessels, *red*), distinguishing human and rat lymphatic vessels (*white arrowheads*) from blood vessels (*white arrows*). LYVE1-positive lymphatic vessels are faintly positive for CD31 too; however, blood vessels are LYVE1 negative. Thus, LYVE1 was used as a lymphatic-specific marker for all further experiments. Cell nuclei are stained with Hoechst (*blue*). *Scale bars* 100 μm

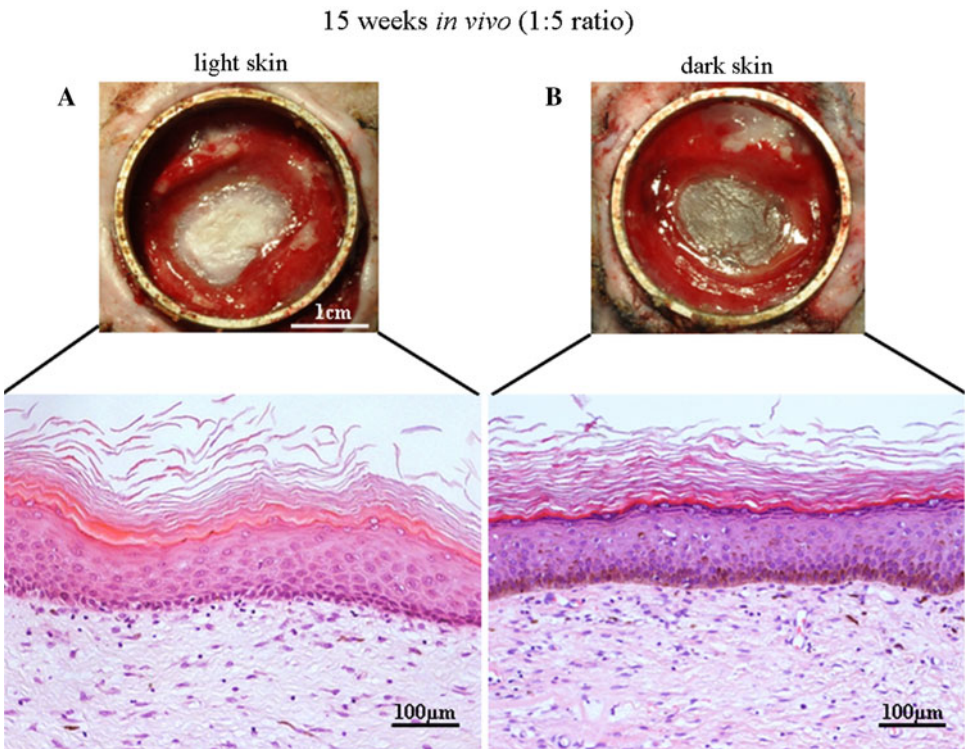

Fig. 2 Tissue-engineered human skin analogs constructed with keratinocytes and melanocytes (1:5 ratio) derived from light or dark donor skin 15 weeks after transplantation. Macroscopic aspect and hematoxylin and eosin staining of light- (**a**) and dark-pigmented (**b**) skin analogs. The constructs both demonstrate a macroscopic and microscopic appearance that, except for the absence of rete ridges and skin appendages, closely resemble normal human light- and dark-pigmented skin. *Scale bars* 100 µm

Rat blood and lymphatic vessel quantification

Vessel profiles in skin analogs were quantified on 6–8 µm thick cryosections double stained for rat CD31/LYVE1 and human CD90. Five random fields at 10× magnification were counted in three different sections of each skin analog after 8 or 15 weeks ($n = 3$–6). Vessel density was expressed as the average number of blood/lymphatic vessels from all fields counted in each skin analog. By double staining for CD31 and LYVE1, it was possible to distinguish and separately quantify $LYVE1^{-}CD31^{+}$ blood vessels and $LYVE1^{+}CD31^{+}$ lymph vessels. All results are reported as mean ± standard deviation (± SD). Statistical analysis was performed with GraphPad Prism 4.0 (Graph Pad software, La Jolla, CA, USA). Comparison between two groups was performed using the unpaired Student's *t* test. Results were considered significant with a $P < 0.05$.

Results

Analysis of normal human and rat skin

Native human and rat skin show specific differences, as demonstrated by a hematoxylin and eosin staining (Fig. 1a, b). In comparison to human foreskin (Fig. 1a), rat back skin (Fig. 1b) is composed of less epidermal layers. It also contains hair follicles and sebaceous glands throughout the dermis. To show the presence of human fibroblasts in the dermal compartment of human skin, we used a human-specific anti-CD90 antibody, which does not stain rat fibroblasts (green, Fig. 1c, d). Human and rat blood vessels, specifically labeled with the anti-human or -rat CD31 antibody (red, Fig 1c, d), were very abundant in the dermis of both species.

To distinguish lymphatic vessels from blood vessels in the skin, we used an antibody to stain LYVE1, a lymphatic endothelium-specific marker (green, Fig. 1e, f). Both human and rat blood vessels were LYVE1 negative; however, lymphatic vessels also showed a faint CD31 staining.

Macroscopic appearance and epidermal structure of human light- and dark-pigmented skin analogs

Eight weeks after transplantation the reconstructed human skin analogs from light- and dark-pigmented donor skin showed a strong resemblance to the donor skin regarding color and structure, independent of which melanocyte/keratinocyte ratio (1:1, 1:5, 1:10) was used (data not shown). Pigmentation was homogenous throughout the entire transplant of all specimens. Also, 15 weeks after transplantation, light- and dark-pigmented skin analogs prepared with a melanocyte/keratinocyte ratio of 1:5 showed macroscopically a light and dark aspect with homogenous pigmentation (Fig. 2a, b). Microscopically, both skin analogs showed a stratified and cornified epidermis on a cellularized neodermis (Fig. 2a, b). However, a

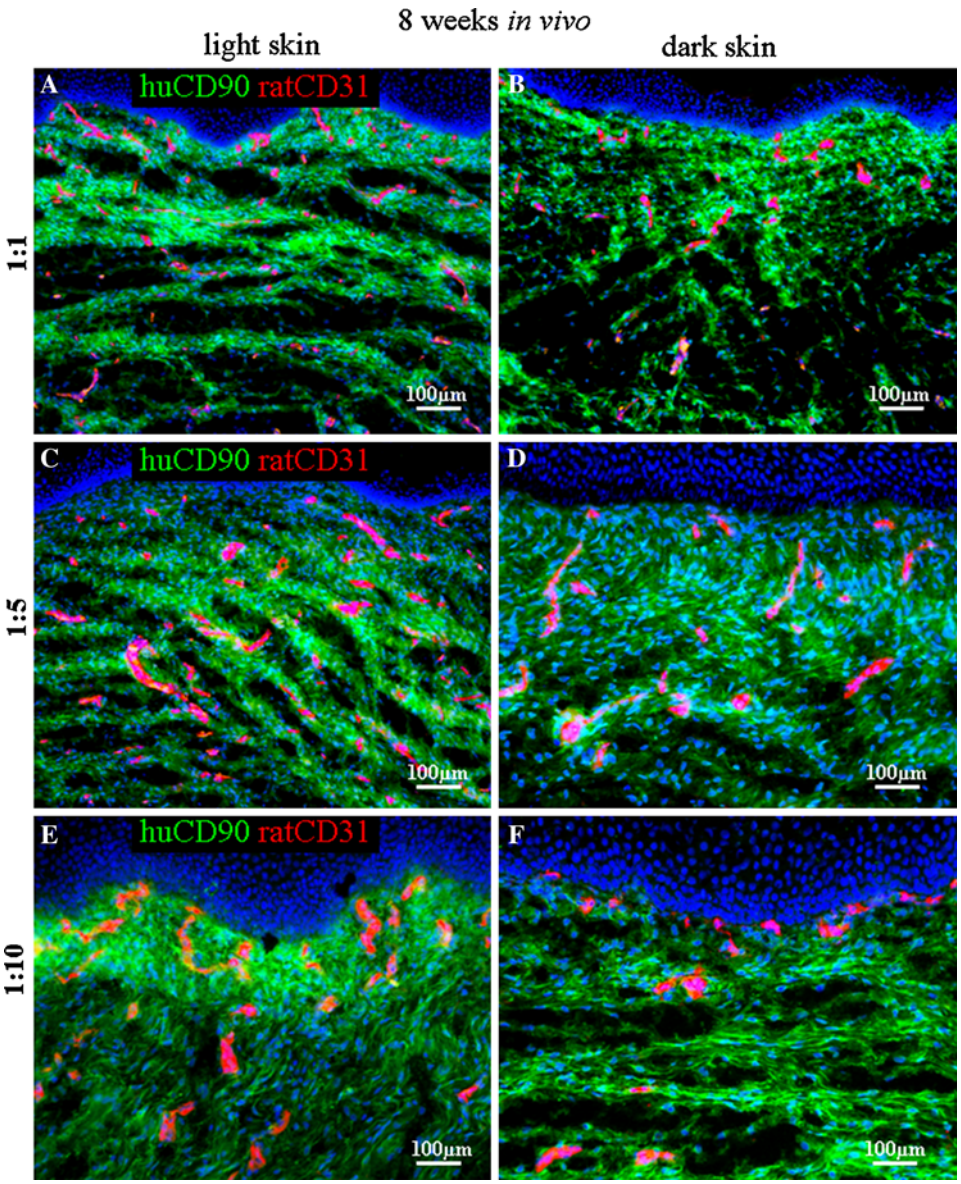

Fig. 3 Host vascularization of light- and dark-pigmented skin analogs (melanocyte/keratinocyte ratio 1:1, 1:5, 1:10) 8 weeks after transplantation. **a, c, e** Rat blood vessels of light skin are stained with an antibody against rat CD31 (*red*). **b, d, f** Rat blood vessels of dark skin are stained with an antibody against rat CD31 (*red*). Human dermal compartment is delineated by an anti-human CD90 staining (*green*), and cell nuclei with Hoechst (*blue*). Light- and dark-pigmented skin analogs show ubiquitous and abundant blood vessels throughout the human CD90-stained neodermis. *Scale bars* 100 µm

noticeable difference between the two analogs was the strongly pigmented basal layer of the dark skin analog (Fig. 2b). Moreover, skin appendages and rete ridges were absent in all engineered skin samples.

Blood vessel patterns of transplanted human tissue-engineered skin analogs

Eight weeks post-transplantation, light- and dark-pigmented skin analogs prepared with different ratios of melanocytes/keratinocytes (1:1, 1:5, 1:10) were excised and analyzed. The human dermal compartment was delineated by an anti-human CD90 staining (green, Fig. 3). The ingrowth of host blood vessels into the human transplants was analyzed using a staining against rat CD31 (red, Fig. 3) and thereafter quantified (Fig. 4).

After 8 weeks, light- and dark-pigmented skin analogs were entirely vascularized showing blood vessels throughout the human CD90-stained dermal compartment with a dense superficial vascular network underneath the epidermis (Fig. 3). The quantification revealed that the light-pigmented group contained a significantly higher number of blood vessels than the dark-pigmented group (Fig. 4a). However, the overall blood vessel density within the light-pigmented group did not show any obvious differences when varying melanocyte/keratinocyte ratios were used: 50 ± 14 vessels/mm^2 (1:1 ratio); 45 ± 8 vessels/mm^2 (1:5 ratio); 51 ± 8 vessels/mm^2 (1:10 ratio). A similar observation was made within the dark-pigmented group: 31 ± 6 vessels/mm^2 (1:1 ratio); 34 ± 8 vessels/mm^2 (1:5 ratio); 34 ± 11 vessels/mm^2 (1:10 ratio) (Fig. 4a).

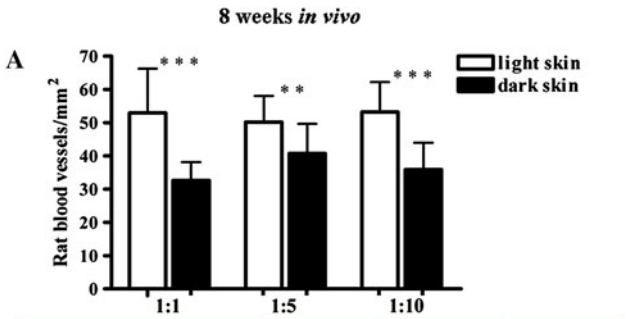

Number of rat blood vessels/mm²	light skin	dark skin	p-value
1:1 (Mean ± SD)	53 ± 13 (N = 3)	33 ± 5 (N = 3)	p < 0.0001
1:5 (Mean ± SD)	50 ± 8 (N = 4)	41 ± 9 (N = 4)	p = 0.003
1:10 (Mean ± SD)	53 ± 9 (N = 3)	36 ± 8 (N = 3)	p < 0.0001

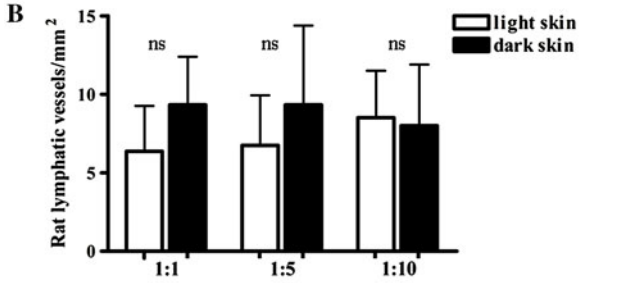

Number of rat lymphatic vessels/mm²	light skin	dark skin	p-value
1:1 (Mean ± SD)	6 ± 3 (N = 3)	9 ± 3 (N = 3)	ns (p = 0.1683)
1:5 (Mean ± SD)	7 ± 3 (N = 4)	9 ± 5 (N = 4)	ns (p = 0.1292)
1:10 (Mean ± SD)	9 ± 3 (N = 3)	8 ± 4 (N = 3)	ns (p = 0.8345)

Fig. 4 The density of rat blood and lymphatic vessels in light- and dark-pigmented skin analogs (melanocyte/keratinocyte ratio 1:1, 1:5, 1:10) 8 weeks after transplantation. **a** Blood vessel (CD31) density of light- (*white bars*) and dark-pigmented analogs (*black bars*). Note a significantly higher number of blood vessels in the light- than the dark-pigmented group. **b** Lymphatic vessel (LYVE1) density of light- (*white bars*) and dark-pigmented analogs (*black bars*). Of note, lymphatic vessel ingrowth occurred at a much lower density as compared to blood vessels, regardless of the pigmentation pattern. Table shows values as the mean (± SD) number of rat blood (**a**)/lymphatic (**b**) vessels quantified per mm^2. $N = 3$ or 4 for each group

After 15 weeks, significantly fewer blood vessels were detected in both light- and dark-pigmented skin analogs (melanocyte/keratinocyte ratio 1:5). The light-pigmented analogs contained 23 ± 10 vessels/mm^2 and the dark-pigmented analogs 25 ± 6 vessels/mm^2 (Figs. 5a, b, 6a).

Lymphatic vessel patterns of transplanted human tissue-engineered skin analogs

Eight weeks after transplantation, the human skin analogs were analyzed for the presence of lymphatic, LYVE1-positive, vessels in the human CD90-stained neodermis and quantified (Fig. 4b). The lymphatic vessels were randomly distributed throughout the human dermal compartment, but were rare in close proximity to the dermo-epidermal junction. They displayed an irregular shape and were slightly larger in diameter than blood capillaries. Moreover, ingrowth was established 5 weeks post-transplantation as compared to blood vessel networks, which were already completely established after 3 weeks in vivo (data not shown).

After 8 weeks, we did not detect any statistically significant difference in the lymphatic vessel densities between varying melanocyte/keratinocyte ratios of light- [6 ± 3 vessels/mm^2 (1:1 ratio); 7 ± 3 vessels/mm^2 (1:5 ratio); 9 ± 3 vessels/mm^2 (1:10 ratio)] and dark-pigmented group [9 ± 3 vessels/mm^2 (1:1 ratio); 9 ± 5 vessels/mm^2 (1:5 ratio); 8 ± 4 vessels/mm^2 (1:10 ratio)]. Of note, they occurred at a much lower density as compared to blood vessels (Fig. 4b).

The number of lymphatic vessels did not change after 15 weeks post-transplantation and was comparable to the amount at 8 weeks in both light- (7 ± 3 vessels/mm^2) and dark-pigmented skin analogs (9 ± 4 vessels/mm^2) (both 1:5 ratio) (Figs. 5c, d, 6b).

Discussion

To the best of our knowledge, this is the first study investigating the blood and lymphatic vessel patterns in differentially pigmented human tissue-engineered skin analogs at 8 and 15 weeks after transplantation. In particular, we analyzed quantitative differences in revascularization patterns between light- and dark-pigmented skin analogs. Overall, our study demonstrates distinctly disparate blood vessel densities in the early wound-healing stages at 8 weeks post-transplantation between the light- and the dark-pigmented groups. Interestingly, this clear differences can no longer be observed at a later stage, namely at 15 weeks post-transplantation. Of note, these differences cannot be seen regarding lymph vessel ingrowth. Some aspects deserve to be addressed in more detail.

The fact that we observe a disparate vascularization pattern between light- and dark-pigmented constructs 8 weeks after transplantation, with a significantly higher amount of blood vessels in the light- compared to the dark-pigmented skin analog group, is clearly surprising. Little is known about differences concerning blood and/or lymphatic vessel densities in light and dark-pigmented human skin. What has already been described is that the facial skin of dark-pigmented individuals contains a higher density of superficial blood vessels than the facial skin of light-pigmented persons [8]. Of note, dark skin is less susceptible to different chemical irritants, most probably due to decreased blood vessel reactivity and therefore less cutaneous blood

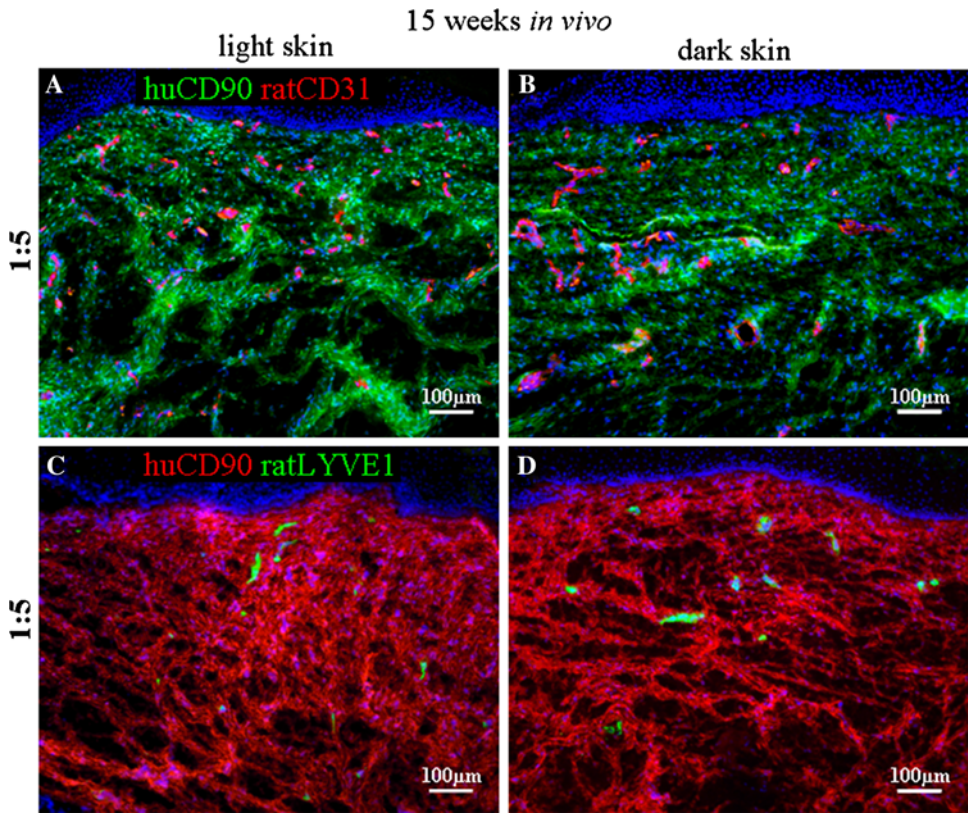

Fig. 5 Host blood and lymphatic vessels in light and dark skin analogs (melanocyte/keratinocyte ratio 1:5) 15 weeks after transplantation. Rat blood vessels of light- (**a**) and dark-pigmented (**b**) skin analogs are stained with an antibody against rat CD31 (*red*). Differentially pigmented skin analogs show similar blood vessel patterns throughout the human CD90-stained neodermis (*green*). Lymphatic vessels of light (**c**) and dark (**d**) skin analogs stained with LYVE1 (*green*) appear at much lower density in human CD90-dermal compartment (*red*) as compared to blood vessels. Cell nuclei are stained with Hoechst (*blue*). *Scale bars* 100 µm

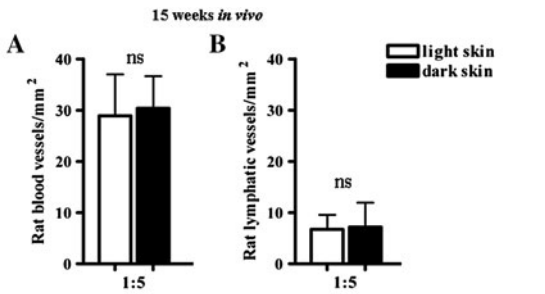

Number of rat blood vessels/mm²	light skin	dark skin	p-value
1:5 (Mean ± SD)	29 ± 8 (N = 6)	30 ± 6 (N = 3)	ns (p = 0.6428)

Number of rat lymphatic vessels/mm²	light skin	dark skin	p-value
1:5 (Mean ± SD)	7 ± 3 (N = 6)	8 ± 4 (N = 3)	ns (p = 0.7116)

Fig. 6 The density of rat blood and lymphatic vessels in light- and dark-pigmented skin analogs (1:5 ratio) 15 weeks after transplantation. **a** Patterns of blood vessel (CD31) in light (*white bars*) and dark analogs (*black bars*) do not reveal any statistically significant difference. **b** Lymphatic vessel (LYVE1) patterns of light (*white bars*) and dark analogs (*black bars*) are comparable and appear at lower density than those of blood vessels. Table show values as the mean (± SD) number of rat blood (**a**)/lymphatic (**b**) vessels quantified per mm^2. $N = 3$ or 4 for each group

flow [9–12]. Our results from 8 weeks after transplantation do not demonstrate a vascularization pattern reflecting this distinct physiological morphology, but rather show the opposite. We hypothesize, that this time point might be too early for skin analogs to show distinct differences as seen in a physiological, i.e., homeostatic situation. Another explanation could be that the differences between dark and light facial skin reported by Montagna et al. [8] might simply not be present in light and dark foreskins as used in our study, because these cells exhibit diverse angiogenic characteristics. Indeed, when analyzing native light and dark foreskin samples, we were not able to detect any apparent differences regarding blood vessels or VEGFA expression patterns (data not shown). Nonetheless, the fact that we observe significant differences in the early, i.e., probably not yet homeostatic, vascular pattern between light- and dark-pigmented skin analogs, suggests that intrinsic signals stemming from keratinocytes, melanocytes, or fibroblasts must be responsible for this transient phenomenon.

Interestingly, 15 weeks post-transplantation no more differences could be detected in the number of vessels present in light and dark grafts. We propose the following interpretation for this change from 8 to 15 weeks. Shortly after transplantation, skin tissue needs to be quickly re-vascularized to ensure cell survival and adequate integration of the transplant into the host tissue [17, 18]. Later, as the graft matures and reaches the remodeling stage, the initially needed, but now redundant, vascular networks are reduced [19, 20].

Of note, although we do notice the described, temporary difference in the vascularization dynamics, all transplants exhibit an apparently competent capillary network within the dermal compartment, ensuring survival and, presumably, also supporting maturation of the dermo-epidermal skin analogs.

Regarding lymphatic vessels, we observe an equal density at 8 and 15 weeks after transplantation. However, their ingrowth occurs later and the number of lymphatic vessels is clearly less compared to blood vessels. Interestingly, an abundant rat blood capillary network can be identified in the dermal compartment as early as 3 weeks post-transplantation, whereas the beginning of lymphatic vessel ingrowth in our skin analogs was seen only 5 weeks after transplantation (data not shown). It is reasonable to argue that the establishment of a rapid vascular supply within the transplanted skin has the highest priority with regard to immediate graft take and long-term survival, and therefore occurs earlier than lymphatic vessel ingrowth. Of note, Nogami et al. [21] followed the recovery of lymphatic vessels in rat skin incision wounds up to 12 weeks and found that lymphatic vessels were not present in the wound area, but only in the surrounding intact tissue. In contrast, we observed that lymphatic vessels regenerated ubiquitously and abundantly in the dermis of our skin analogs already 5 weeks after transplantation. Furthermore, previous reports showed that lymphatic regeneration across scar tissues is severely impaired and that fibrosis in a wound can be directly responsible for lymphedema formation due to reduced lymphatic endothelial cell proliferation and abnormal lymphatic microarchitecture [22, 23]. In light of the above, our findings are particularly important with regard to our planned clinical application of laboratory-engineered skin substitutes. It appears tenable that a competent lymphatic vessel supply will also develop when our skin substitutes are autologously transplanted onto human patients.

In summary and conclusion, this appears to be the first article demonstrating that differently pigmented human tissue-engineered dermo-epidermal skin analogs show a near physiological ingrowth of both blood and lymphatic vessels in a rat model. Further, our results suggest that different cells, especially keratinocytes, melanocytes, and fibroblasts of light- and dark-pigmented skin analogs seem to orchestrate temporarily disparate vascularization patterns. It appears likely that favorable blood and lymphatic vessels ingrowth dynamics take place when autologous tissue-engineered skin analogs are transplanted onto human patients.

Acknowledgments This work was financially supported by the EU-FP6 project EuroSTEC (soft tissue engineering for congenital birth defects in children: contract: LSHB-CT-2006-037409), by the EU-FP7 project EuroSkinGraft (FP7/2007-2013: grant agreement nr 279024), the EU-FP7 (MultiTERM, grant agreement nr 238551), and the Clinical Research Priority Programs (CRPP) of the Faculty of Medicine of the University of Zurich. We are particularly grateful to the Gaydoul Foundation and the sponsors of "DonaTissue" (Thérèse Meier and Robert Zingg) for their generous financial support and interest in our work.

Conflict of interest The authors declare that they have no conflict of interest.

References

1. Braziulis E, Diezi M, Biedermann T, Pontiggia L, Schmucki M, Hartmann-Fritsch F, Luginbuhl J, Schiestl C, Meuli M, Reichmann E (2012) Modified plastic compression of collagen hydrogels provides an ideal matrix for clinically applicable skin substitutes. Tissue Eng Part C Methods 18:464–474
2. Biedermann T, Bottcher-Haberzeth S, Klar AS, Pontiggia L, Schiestl C, Meuli-Simmen C, Reichmann E, Meuli M (2013) Rebuild, restore, reinnervate: do human tissue engineered dermo-epidermal skin analogs attract host nerve fibers for innervation? Pediatr Surg Int 29:71–78
3. Pontiggia L, Klar A, Bottcher-Haberzeth S, Biedermann T, Meuli M, Reichmann E (2013) Optimizing in vitro culture conditions leads to a significantly shorter production time of human dermo-epidermal skin substitutes. Pediatr Surg Int 29:249–256
4. Pontiggia L, Biedermann T, Meuli M, Widmer D, Bottcher-Haberzeth S, Schiestl C, Schneider J, Braziulis E, Montano I, Meuli-Simmen C, Reichmann E (2009) Markers to evaluate the quality and self-renewing potential of engineered human skin substitutes in vitro and after transplantation. J Invest Dermatol 129:480–490
5. Bottcher-Haberzeth S, Klar AS, Biedermann T, Schiestl C, Meuli-Simmen C, Reichmann E, Meuli M (2013) "Trooping the color": restoring the original donor skin color by addition of melanocytes to bioengineered skin analogs. Pediatr Surg Int 29:239–247
6. Plensdorf S, Martinez J (2009) Common pigmentation disorders. Am Fam Physician 79:109–116
7. Weigand DA, Haygood C, Gaylor JR (1974) Cell layers and density of Negro and Caucasian stratum corneum. J Invest Dermatol 62:563–568
8. Montagna W, Carlisle K (1991) The architecture of black and white facial skin. J Am Acad Dermatol 24:929–937
9. Marshall EC (1989) Racial differences in the presentation of chronic open-angle glaucoma. J Am Optom Assoc 60:760–767
10. Wedig JH, Maibach HI (1981) Percutaneous penetration of dipyrithione in man: effect of skin color (race). J Am Acad Dermatol 5:433–438
11. Berardesca E, Maibach HI (1988) Sodium lauryl sulfate induced cutaneous irritation—comparison of white and Hispanic subjects. Con Dermat 19:136–140
12. Berardesca E, Maibach HI (1988) Racial-differences in sodium lauryl sulfate induced cutaneous irritation—black and white. Con Dermat 18:65–70
13. Biedermann T, Pontiggia L, Bottcher-Haberzeth S, Tharakan S, Braziulis E, Schiestl C, Meuli M, Reichmann E (2010) Human eccrine sweat gland cells can reconstitute a stratified epidermis. J Invest Dermatol 130:1996–2009
14. Schneider J, Biedermann T, Widmer D, Montano I, Meuli M, Reichmann E, Schiestl C (2009) Matriderm versus integra: a comparative experimental study. Burns 35:51–57
15. Bottcher-Haberzeth S, Biedermann T, Schiestl C, Hartmann-Fritsch F, Schneider J, Reichmann E, Meuli M (2012) Matriderm(R) 1 mm versus integra(R) single layer 1.3 mm for one-

step closure of full thickness skin defects: a comparative experimental study in rats. Pediatr Surg Int 28:171–177
16. Bottcher-Haberzeth S, Biedermann T, Pontiggia L, Braziulis E, Schiestl C, Hendriks B, Eichhoff OM, Widmer DS, Meuli-Simmen C, Meuli M, Reichmann E (2013) Human eccrine sweat gland cells turn into melanin-uptaking keratinocytes in dermo-epidermal skin substitutes. J Invest Dermatol 133:316–324
17. Bhora FY, Dunkin BJ, Batzri S, Aly HM, Bass BL, Sidawy AN, Harmon JW (1995) Effect of growth factors on cell proliferation and epithelialization in human skin. J Surg Res 59:236–244
18. Martin P (1997) Wound healing—aiming for perfect skin regeneration. Science 276:75–81
19. Gurtner GC, Werner S, Barrandon Y, Longaker MT (2008) Wound repair and regeneration. Nature 453:314–321
20. Blanpain C, Fuchs E (2009) Epidermal homeostasis: a balancing act of stem cells in the skin. Nat Rev Mol Cell Biol 10:207–217
21. Nogami M, Hoshi T, Arai T, Toukairin Y, Takama M, Takahashi I (2009) Morphology of lymphatic regeneration in rat incision wound healing in comparison with vascular regeneration. Leg Med (Tokyo) 11:213–218
22. Warren AG, Slavin SA (2007) Scar lymphedema: fact or fiction? Ann Plast Surg 59:41–45
23. Avraham T, Clavin NW, Daluvoy SV, Fernandez J, Soares MA, Cordeiro AP, Mehrara BJ (2009) Fibrosis is a key inhibitor of lymphatic regeneration. Plast Reconstr Surg 124:438–450